WILEY | Hindawi

Research Article

Loss Minimization of Distribution Systems by Coordinated Operation of Battery and EVs in the Presence of DGs

Kartik Iyer,[1] Snehith Perumalla,[1] Menakuru Sai Eswar Reddy,[1] Krishnan Narayanan [ID],[1] Natarajan Prabaharan [ID],[1] Gulshan Sharma [ID],[2] and Tomonobu Senjyu [ID][3]

[1]*Department of EEE, SASTRA Deemed University, Thanjavur, Tamilnadu, India*
[2]*Department of Electrical Engineering Technology, University of Johannesburg, Johannesburg, South Africa*
[3]*Department of EEE, University of Ryukyus, Nishihara, Okinawa, Japan*

Correspondence should be addressed to Krishnan Narayanan; narayanan.mnit@gmail.com

The rapidly increasing demand for electrical power and difficulties in providing the same using traditional power generating sources provide a motivation to integrate distributed generator (DG) in the radial distribution network. In this work, the optimal arrangement of DG using genetic algorithm (GA) is obtained based on fixed penetration level (PL). The state of charge (SoC) value for each hour before placing the battery based on the demand was estimated, then battery will be placed in the optimal location of the fixed capacity. This will help in reducing the power loss and simultaneous improvement of voltage profile of the network. Furthermore, electric vehicle (EV) is incorporated in the system. In the presence of EV, the loads are variable due to the charging and discharging of batteries in the EV. The variation of network power losses in the presence of EVs along with DGs and battery have been investigated on standard 33 and 69 bus systems for 2 different topologies and 2 different loading scenarios.

1. Introduction

Demand for electrical power increases rapidly in the country; at the same time, there are difficulties such as high power losses, low voltage stability index, and high voltage drop. This provides a motivation to integrate distributed generator (DG) into the radial distribution network which are predominantly renewable energy resources. The study of [1] introduces a power management method with comprehensive linearized model for HESS optimal sizing, technology selection, and wind-HESS power dispatching. In [2], a novel combined genetic algorithm (GA) and particle swarm optimization (PSO) is presented for optimal location and sizing of DG on distribution systems, whereas paper [3] proposes an optimization framework with the objective of maximizing the installed capacity of distributed generation subject to network operational constraints. The study of [4] presents an ODGA and NR processes incorporated to improve the voltage stability and loss profile of the distribution system considering probabilistic loads and DGs which are operated at varying power factors, and the study of [5] presents a formulation for the analysis of DER penetration and placement on system losses and voltage profile in probabilistic framework. The study of [6] provides the improved decomposition based evolutionary algorithm (I-DBEA) is used for the selection of optimal number, capacity, and site of DG in order to minimize real power losses and voltage deviation and to maximize the voltage stability index. Rider optimization algorithm (ROA) is suggested in [7] to find the optimal placement of photovoltaic (PV) and wind turbine (WT) based DGs. The main aim is minimizing the total power losses. The study of [8] examines the effect of demand response (DR) after integration of renewable resources based DGs in the distribution system and [9] proposes the optimal installation of multiple DGs to achieve higher reliability using cat swarm optimization.

In the study of [10], the objective is to find optimal location of BSSs in a MG with micropumped hydro storage (PHS), photovoltaic, wind, and geothermal units, while reactive power dispatch and all network constraints are

considered by AC optimal power flow. The effect of BSS capacity and maximum charging/discharging power, BSS to MG link capacity, PHS capacity, and maximum power of PHS unit on MG operation and optimal BSS location are investigated. The study of [11] proposes a novel set of formulations to determine the optimal BES size, technology, depth of discharge (DoD), and replacement year considering its technical characteristics, service life, and capacity degradation to minimize the MG scheduling total cost and improve the precision and economic feasibility of the BES sizing method. In the study of [12], a new optimal operation approach is proposed for the BESs. The proposed new model determines the optimal charging, discharging, and exchange decisions for the battery stock throughout the day taking into consideration the customers' arrivals, the variations in the grid price, the grid connection limitations, and the self-degradation of the batteries.

In [13], a new methodology for optimal planning of charging stations (CSs) along with capacitors is presented. Here, parking lot and capacitor allocation is suggested for congestion management along with reactive power compensation. The study of [14] research helps in planning the optimum utilization of the existing infrastructure. The planning of electric vehicle (EV) infrastructure is analyzed by considering various loads such as static, dynamic, and heuristic on balanced radial distribution system (BRDS). The study of [15] presents the optimal positioning EVs in the system with and without presence of DGs installed in the system using GA. The study of [16] articulated sizing and placement of DG in the distribution system and to support the grid with the help of particle swarm optimization (PSO). After that the battery storage system is placed, and the operation of the battery in accordance with the state of charge (SoC) is also presented [17]. This study focuses on developing a mathematical model for uncertainty constrained battery swapping station optimal operation considering random customer demand for fully charged batteries and available batteries to reduce its operating cost through demand shifting and energy sell back. The study of [18] presents a grid-connected solar-wind hybrid system with an EV charging station to supply the electrical load demand of a small shopping complex located in a university campus in India. From the perspective of grid stability, the study of [19] presents the planning and operation problem by determining the load profile of EVCS. A coordinated novel charging strategy is used for the determination of the load profile of EVCS constrained by both grid-to vehicle (G2V) and vehicle-to-grid (V2G) rule sets.

The study of [20] presents a new method to solve the network reconfiguration problem in the presence of distributed generation (DG) with an objective of minimizing real power loss and improving voltage profile in distribution system. A meta heuristic harmony search algorithm (HSA) is used to simultaneously reconfigure and identify the optimal locations for installation of DG units in a distribution network. Sensitivity analysis is used to identify optimal locations for installation of DG units. The study of [21] proposes empirical mode decomposition based adaptive reclosing technique which can sense the exact instant of fault clearance and modify the prefixed dead time to an adaptive value. The study of [22] a mixed-integer linear programming model for feeder reconfiguration is presented considering the customer's behaviors in the IoT environment.

The work aims to integrate the DGs and EVs in the standard IEEE bus systems to minimize power loss and voltage profile improvement. This work presents an overview of DGs in the distribution network. The proper placement and sizing of DG is a significant task. Also, the presence of an electric vehicle (EV) in the distribution system tends to change the existing load pattern and various combinations of load pattern of EVs and DGs has to be investigated. Hence, this also gives more impetus to analyze the performance of the system under such varying conditions. Genetic algorithm (GA) is used to find the locations and sizes of distributed generators (DGs). After placement of DG, the same GA is used to filter out the locations for the battery of certain size. Once the battery locations are filtered out, the optimal location for the battery to be placed is determined. Since, battery is not placed separately in the distribution system, DGs are placed in the optimal locations which are found using the GA and LFA with specific sizes. Henceforth, using the same LFA code, the losses are found out for the case where battery and DGs are incorporated in the system. Furthermore, for more loss minimization, electric vehicle (EV) is introduced in the system. It is placed in the system with varying the sizes because EV charges and discharges with respect to time and the losses are found out for the same. Finally, EV is incorporated with both the battery and DGs for the further loss minimization in the system, and LFA is hence used for finding out the losses in the distributed systems. The above-given process is performed for two different topologies and two different loading scenarios. The objective of the present work is to evaluate and reduce the power losses in the presence of DGs, BESS, and EVs for each hour under varying load conditions. The major contributions of this work are as follows:

(i) Installing the optimal number of DGs simultaneously based on the Penetration Level (PL)

(ii) Determining the battery operation based on hourly availability of power from DGs and the SoC level

(iii) Incorporation of EVs, and their impact on the system performance based on availability of power from DGs and the battery operation.

2. Problem Formulation

Heuristic algorithms are the best assets when it comes to optimization problems. There are several algorithms; one among those algorithms is genetic algorithm. What make it different from other conventional algorithms is GA searches simultaneously from a given population. Therefore, the solutions obtained through GA avoid being trapped in local optima.

The distributed generator (DG) is used to reduce the power losses in the system by supplying optimal power to the system by placing the DGs in optimal location having optimal sizes. These optimal sizes and locations are found using

GA. The optimal number of DGs required is 3 according to the [6]. Asynchronous generator is used here as DG.

Penetration level (PL) is used to estimate how much the power is consumed by the load from the grid and power needed from DGs and EVs to fulfill the demand. The effective sizes of DGs are determined based on the *PL* obtained through the following equation:

$$PL = \frac{P_{DG}}{P_{DG} + P_{grid}}, \tag{1}$$

where PL—penetration level, P_{DG}—real power generated by DGs, and P_{grid}—the real power supplied by the grid to the loads in the network.

PL is usually considered lesser than 50% as with higher values the DG power will dominate the real power supplied by the grid.

The presence of DGs will minimize the power loss in the system and the effect of the DGs on the loss reduction (LR) can be computed by the following equation:

$$LR = \frac{loss\ without\ DG - loss\ with\ DG}{loss\ without\ DG}. \tag{2}$$

The following equations ensure the constraints for optimal location of DGs in the system:

$$V_{low} \leq V_t \leq V_{high}, \\ S_{line} \leq S_{high}, \tag{3}$$

where V_{low} is the minimum voltage to be maintained at the buses and V_{high} is the maximum voltage to be maintained at the buses. The values of V_{low} and V_{high} are considered as 0.95 p.u. and 1.05 p.u. S_{line} is the power flow in the line.

2.1. Genetic Algorithm.
Genetic algorithm works by initializing the random solutions to the given optimization problem through a population of individuals. They are organized on the basis of the fitness obtained through the given objective function.

2.1.1. Initial Population.
An individual solution contains PL, location index, and the type of DG represented by x_1, x_2, and x_3, respectively. Since x_2 is the location index, it ranges from 1 to L, and L is the highest location index of respective bus system. If $x_3 = 1$, then the type of *DG* is asynchronous generator, for $x_3 = 2$, the generator is synchronous, and $x_3 = 3$ represents induction generator. The population matrix X for "n" number of individual is given by the following equation:

$$X = \begin{bmatrix} x_{11} & x_{12} & x_{13} \\ \cdot & \cdot & \cdot \\ \cdot & \cdot & \cdot \\ x_{n1} & x_{n2} & x_{n3} \end{bmatrix}. \tag{4}$$

The ith individual is represented as

$$x_i = [x_{i1} x_{i2} x_{i3}]. \tag{5}$$

2.1.2. Selection.
If two individuals x_i and x_j are selected from population matrix X, c_i, and c_j are the values returned by the objective function. P is the set of all the parents that have a chance of reproduction, then

$$X_i \in P, if\ c_i <= c_j. \tag{6}$$

2.1.3. Reproduction.
From possible parents P, p_i and p_j are selected parents:

$$p_i = \begin{bmatrix} p_{i1} & p_{i2} & p_{i3} \end{bmatrix}, \\ p_j = \begin{bmatrix} p_{j1} & p_{j2} & p_{j3} \end{bmatrix}. \tag{7}$$

2.1.4. Crossover.
Let k be the selected crossover point, $1 <= k <= 3$, and let o_i and o_j be the two crossover children from parents' p_i and p_j:

$$o_i = \begin{bmatrix} P_{i1} \ldots P_{ik} \ldots P_{jk+1} \ldots P_{j3} \end{bmatrix}, \\ o_j = \begin{bmatrix} P_{j1} \ldots P_{jk} \ldots P_{ik+1} \ldots P_{i3} \end{bmatrix}. \tag{8}$$

Furthermore, the o_i and o_j acts as parent for subsequent iteration. This process continues until convergence is reached or the iterations are terminated.

2.1.5. Mutation.
It is the process of retrieving lost characteristics or property from the parent. Given a population X, a mutant child "m" is procured by choosing any random individual x_i. One of the genes of x_i is randomly chosen and modified.

2.1.6. Battery Energy Storage System.
The BESS size is taken to be constant 600 kW in this study and the operation of battery is studied in this work and the constraints are given in equation (10). The limits for SoC is assumed as 0.2 and 0.8 p.u. The initial SoC is taken as 0.95 p.u. [16]. The state of charge (SoC) of the energy storage system is calculated by the given equations (11) and (12) under charging and discharging conditions. The efficiencies are taken as 90%. Under discharging mode, the battery power is negated from the demand and corresponding battery power can be calculated by equation (13). The battery power is added to the load/demand when it is in charging mode which is because the battery draws power from either grid or the renewable energy source. In equation (10), SoC_{min} is minimum state of charge and SoC_{max} is maximum state of charge. In equations (11) and (12), SoC (y) is SoC in present hour and SoC (y − 1) is SoC in previous hour, "E" is energy of the battery in kWh and ∂_y is the time interval. The battery charges at rated power of battery which is initially the difference between the generation and the load. The specification of the battery bank is given below referred from [10].

$$SoC_{\min} \leq SoC(y) \leq SoC_{\max}, \tag{9}$$

$$SoC(y) = SoC(y-1) + P_{\text{batt}}(y) * \partial_y * \eta_c, \tag{10}$$

$$SoC(y) = SoC(y-1) - P_{\text{batt}}(y) * \partial_y * \eta_d, \tag{11}$$

$$P_{\text{batt}}(y) = SoC(y) * E, \tag{12}$$

$$o_j = \left[P_{j1} \ldots P_{jk} \ldots P_{ik+1} \ldots P_{i3} \right], \tag{13}$$

where E = Energy of the battery, ∂_y = Time interval, η_d = Discharging efficiency, η_c = Charging efficiency, $SoC(y)$ = State of Charge in present hour, $SoC(y-1)$ = State of Charge in previous hour, and P_{batt} = Output Power of the battery.

2.1.7. Electric Vehicle.

Figure 1 shows the usage pattern of EV in 24 hour duration. The capacity of EV is taken as positive when in discharge mode and negative when in charging mode. The presence of EV is also considered along with the existing load conditions [10].

2.1.8. Loading Conditions.

Two different loading scenarios are considered for the analysis in the present work and the load profile is shown in Figure 2.

2.1.9. Topology.

Topology 1 is the general architecture of nodes and buses in the distributed system. For 33 bus system and 69 bus system, the line number 33, 34, 35, 36, and 37 and line number 69, 70, 71, 72, and 73, respectively, are opened. The power loss in this topology is considered as base case. In topology 2, the line number 7, 9, 14, 32, and 37 and the line number 14, 57, 61, 69, and 70 are opened for 33 bus system and 69 bus system, respectively. Topology 2 is considered to have the least power loss among all the combinations possible according to [20]. The single line diagram of the topology 1 and 2 of IEEE 33 bus system is shown in Figures 3 and 4, respectively, and for 69 bus shown in Figures 5 and 6, respectively.

Case 1 Base losses

Case 2 Losses with DGs

Case 3 Losses with DGs and battery

Case 4 Losses with EVs

Case 5 Losses with DGs, battery and EVs

2.1.10. State of Charge of Battery.

The battery operations are classified as "Charging," "Discharging," and "Idle" based on the state of charge (SoC). The function of the battery is dependent on the hourly demand. The SoC is hence calculated using the formula below with the constraints considered. The battery operation status of Scenario 1 and Scenario 2 is shown in Tables 1 and 2, respectively.

The procedure for the entire process is shown as a flowchart in Figure 7.
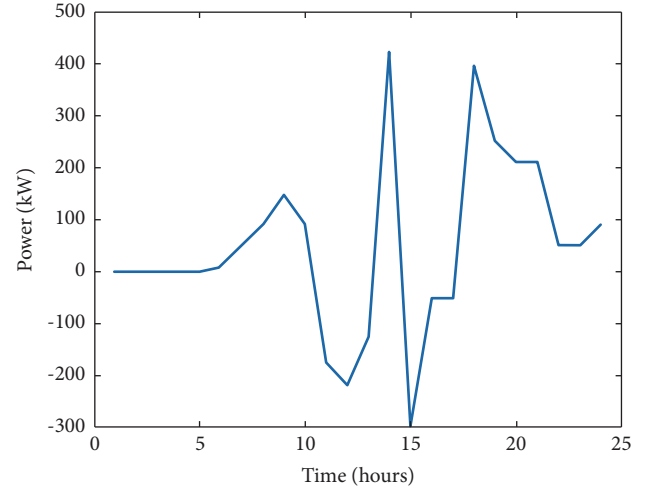
FIGURE 1: EV power vs time plot.
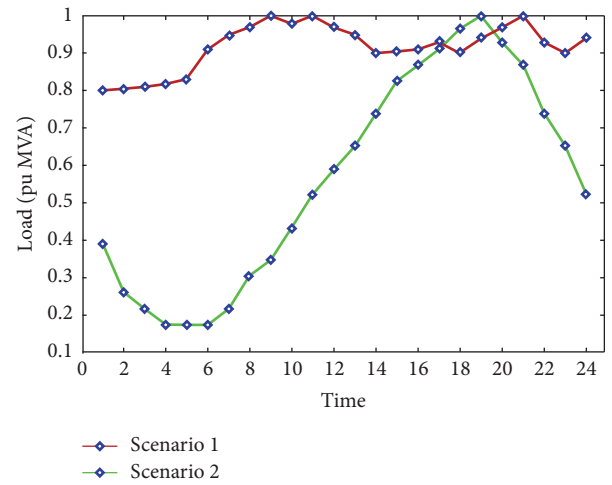
FIGURE 2: Load variation for 24 hour.

3. Results

Power loss is inevitable in transmission lines due to multiple factors which can be reduced by strategically placing DGs and EVs. The following results are found for standard IEEE 33 and 69 bus systems. The optimal number of locations are three which is taken from the paper [20]. GA is used to determine the optimal locations and sizes for the DGs and EVs and found efficient ones with improved voltage profile along with loss reduction, also examined for various combinations of DGs and EVs with two scenarios of different multiplication factors. In this case, mutation is considered to be 5% and crossover is 20%. Penetration level is set at 40% which accounts to 2476.67 kW and 2534.79 kW for standard IEEE 33 and 69 bus systems, respectively. The optimal locations and sizes of DGs are discovered after several GA trials.

For topology 2, the nodes 7, 9, 14, 32, and 37 are opened, and using GA, provided 5% mutation and 20% crossover, with 40% penetration level, the optimal locations and sizes are found out. The above-given operation was carried out for
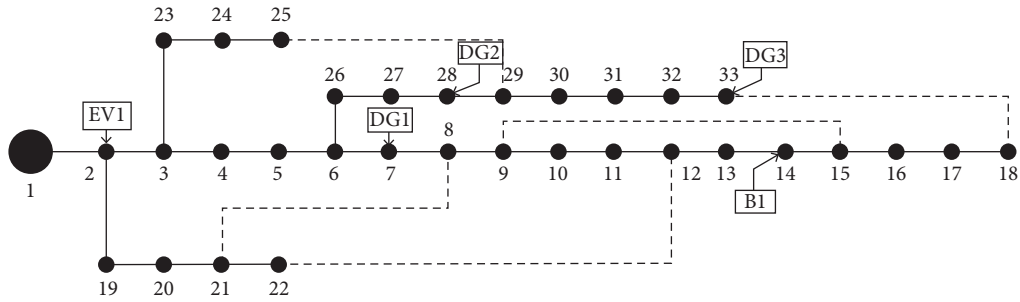
FIGURE 3: Topology 1 of IEEE 33 bus system.
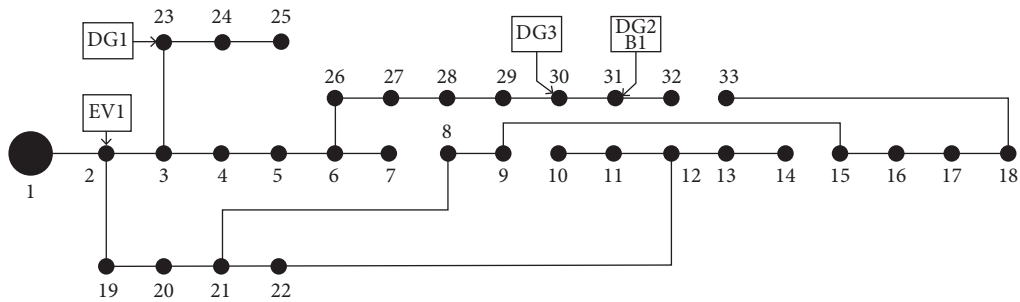
FIGURE 4: Topology 2 of IEEE 33 bus system.
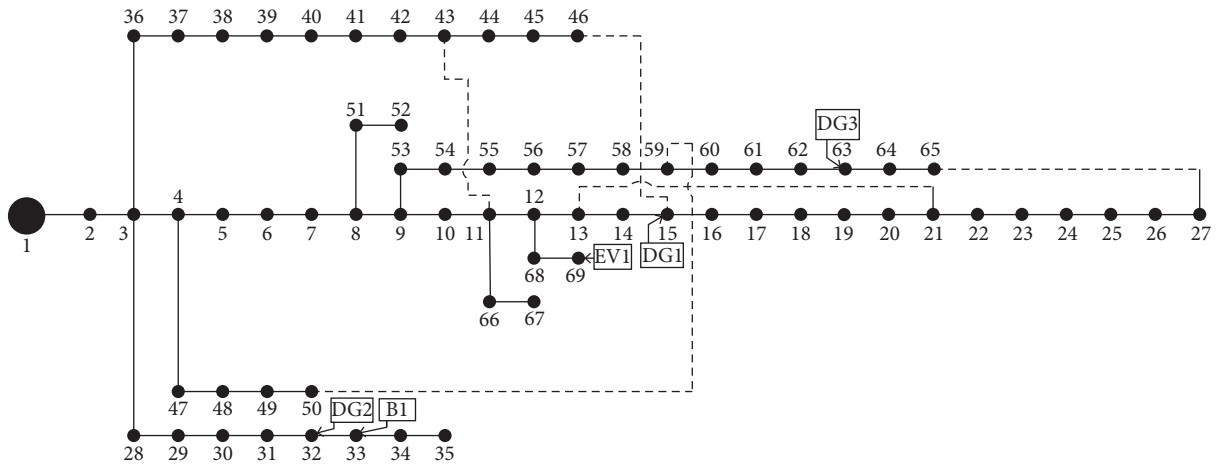
FIGURE 5: Topology 1 of IEEE 69 bus system.

IEEE 33 bus system. Similarly, for IEEE 69 bus system, line number 13, 18, 56, 61, and 73 are opened with the same mutation and crossover values. The optimal locations and sizes of DGs of 33 and 69 bus system for topology 1 and 2 are shown in Tables 3 and 4.

Next crucial step is the placement of battery at its optimal location. In these systems like IEEE 33 bus system and 69 bus system, it is time consuming process to check for each bus for the losses and get the optimal location for the battery. Rather, GA can be used to filter out the bus number which are more sensitive in reducing the losses. The battery used in this project is of size 600 kW. The placement of battery is done in following locations for the 2 topologies as shown in Table 5.

3.1. 33 Bus System.

The power losses for 24 hours are computed for the two different loading scenarios and two different topologies for the 33 Bus system. The results are shown in Tables 6 and 7.

3.1.1. Scenario 1

(1) Topology 1. The losses are high in 9th, 11th, and 21st hours of the day in the presence of maximum amount of load which is 201.9708 kW for each hour. The loss in the presence of DGs is 112.5945 kW for the 9th, 11th, and 21st hours. Here, the losses are reduced by 44.25% by fulfilling the demand. In the next case, the loss in the presence of battery and DGs, for

FIGURE 6: Topology 2 of IEEE 69 bus system.

TABLE 1: Battery operation for scenario 1.

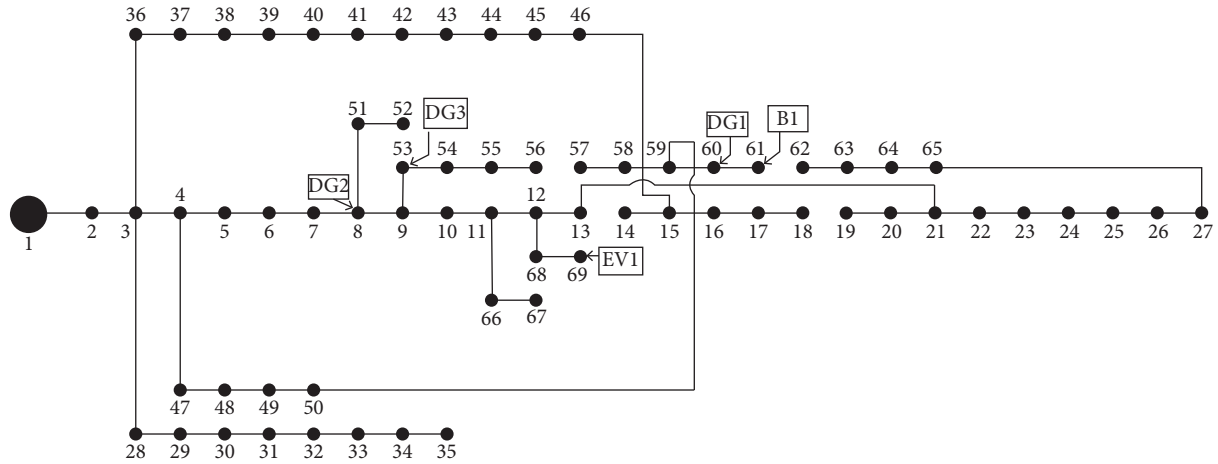| Time (hours)	Demand (p.u.)	SoC (p.u.)	State of battery
1	0.800	0.95	Idle
2	0.805	0.95	Idle
3	0.810	0.95	Idle
4	0.818	0.95	Idle
5	0.830	0.95	Idle
6	0.910	0.94	Discharging
7	0.950	0.89	Discharging
8	0.970	0.83	Discharging
9	1	0.74	Discharging
10	0.980	0.67	Discharging
11	1	0.58	Discharging
12	0.970	0.52	Discharging
13	0.950	0.47	Discharging
14	0.900	0.47	Idle
15	0.905	0.47	Discharging
16	0.910	0.46	Discharging
17	0.930	0.43	Discharging
18	0.900	0.43	Idle
19	0.940	0.40	Discharging
20	0.970	0.33	Discharging
21	1	0.24	Discharging
22	0.930	0.22	Discharging
23	0.900	0.22	Idle
24	0.940	0.22	Idle

TABLE 2: Battery operation for scenario 2.

Time (hours)	Demand (p.u.)	SoC (p.u.)	State of battery
1	0.39	0.95	Idle
2	0.26	0.95	Idle
3	0.22	0.95	Idle
4	0.17	0.95	Idle
5	0.17	0.95	Idle
6	0.17	0.95	Idle
7	0.22	0.95	Idle
8	0.30	0.95	Idle
9	0.35	0.95	Idle
10	0.43	0.95	Idle
11	0.52	0.95	Idle
12	0.59	0.95	Idle
13	0.65	0.95	Idle
14	0.74	0.95	Idle
15	0.83	0.95	Idle
16	0.87	0.95	Idle
17	0.91	0.94	Discharging
18	0.97	0.88	Discharging
19	1	0.79	Discharging
20	0.93	0.76	Discharging
21	0.87	0.79	Charging
22	0.74	0.93	Charging
23	0.65	0.93	Idle
24	0.52	0.93	Idle

9th hour is 88.7445 kW, for 11th hour is 92.9423 kW, and for 21st hour is 105.2599 kW, the losses are decreased by 56.06%, 53.98%, and 48.88%, respectively, where battery is in discharging position because of this condition the losses are decreased. In the case 4, the loss for 9th hour is 202.7022 kW, and for the 11th hour is 201.1506 kW and for the 21st hour is 203.0022 kW. The loss is increased by 0.36% for the 9th hour as EV acts as load for the system and has decreased 0.40% for the 11th hour as EV acts as source here so its loss is decreased and has increased for 21st hour by 0.51% due to EV acts as load for the system. In the subsequent case, when all three sources are integrated to the system, the losses are reduced to 89.1522 kW, 92.4782 kW, and 105.9194 kW for 9th, 11th, and 21st hour. The losses are reduced by 55.85% for 9th hour,

54.21% for 11th hour, and 47.55% for 21st hour which is lesser than the losses when only DG is integrated because either battery or EV acts as source which fulfills the demand for the required hours.

(2) Topology 2. The losses are high in 9th, 11th, and 21st hour of the day in the presence of maximum amount of load which is 98.4633 kW for each hour. The loss in the presence of DGs is 59.387 kW for the 9th hour, 11th hour, and 21st hour. Thereby reducing the losses by 39.68% because DGs are placed such that it can fulfill the demand. In the case 3, the loss in the presence of battery and DGs, for 9th hour is 53.9997 kW, for 11th hour is 54.33 kW, and for 21st hour is 57.4615 kW, the losses are decreased by
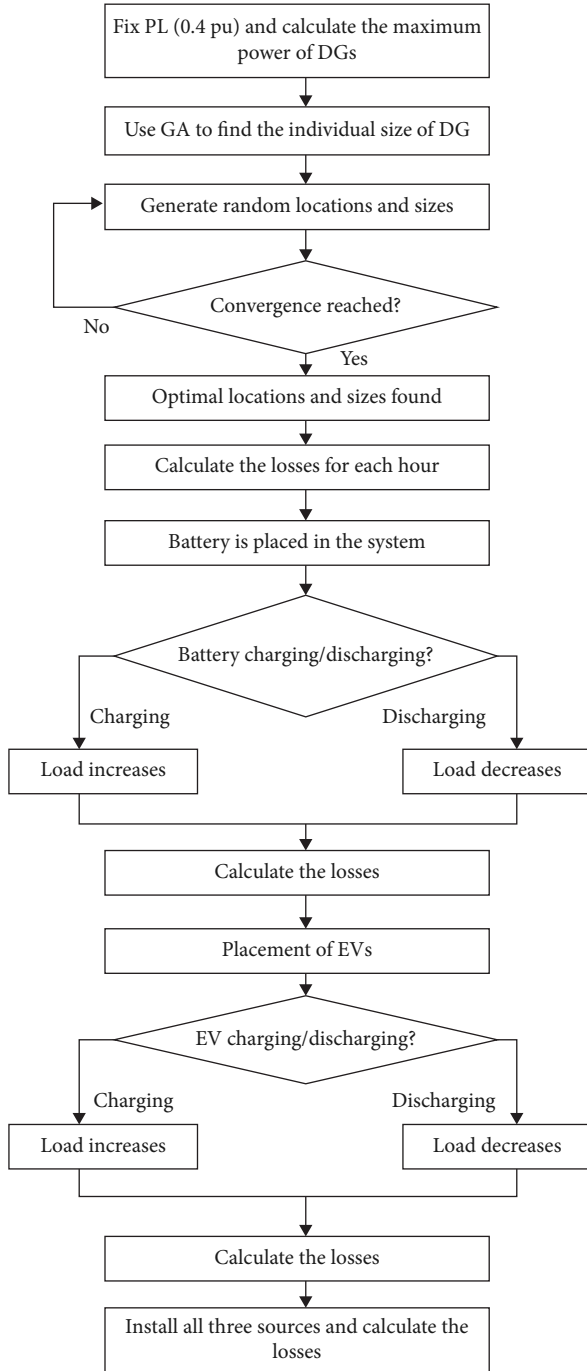
Figure 7: Proposed flow of work.

Table 3: Optimal locations and sizes of DGs for 33-bus.

	Topology 1			Topology 2		
DG locations	7	28	33	23	31	30
DG sizes	340	404	556	350	218	376

Table 4: Optimal locations and sizes of DGs for 69-bus.

	Topology 1			Topology 2		
DG locations	15	33	63	60	8	53
DG sizes	209	164	859	817	194	334

Table 5: Optimal location of battery.

Location	Topology 1	Topology 2
33 bus system	14	31
69 bus system	32	61

45.15%, 44.82%, and 41.64%, respectively. Battery is in charging state in 21st hour because of this condition the losses are decreased and the battery is idle for the 9th and 11th hour. In the next case, only EVs are integrated in the system, then loss for 9th hour is 98.9607 kW, for the 11th hour is 97.9161 kW, and for the 21st hour is 99.167 kW. The loss is increased by 0.50% for the 9th hour as EV acts as load for the system, has decreased 0.55% for the 11th hour as EV acts as source, so the loss is decreased and has increased for 21st hour by 0.71% due to EV acts as load for the system. In the case 5, when all three sources are integrated to the system, the losses are reduced to 54.2562 kW, 54.0439 kW, and 57.9023 kW for 9th, 11th, and 21st hour, respectively. The losses are reduced by 44.89% for 9th hour and 45.11% for 11th hour and 41.19% for 21st hour which are lesser than the losses when only DG alone is integrated, that is because battery acts as source for 21st hour, for remaining hour EV acts as energy source.

3.1.2. Scenario 2

(1) Topology 1. In scenario 2, the losses for each hour for each case is shown in Table 7. The losses are high in 19th hour of the day in absence of DGs due to the presence of maximum amount of load which is 201.9708 kW for that particular hour. The loss in the presence of DGs is 112.5945 kW for the 19th hour. Thereby reducing the loss by 44.25% by supplying the required energy to the load. In the case 3, the loss in the presence of battery and DGs, for 19th hour is 87.7364 kW, the loss is decreased by 56.55% where battery is in discharging position because of this condition the losses are decreased. In the next case, the loss for 19th hour is 203.2045 kW. The loss is increased by 0.61% for the 19th hour as EV acts as load for the system. In the last case, the losses are reduced to 88.4217 kW for 19th hour. The loss is reduced by 56.22% for 19th hour which is lesser than the losses when only DG is integrated battery acts as energy source for 19th hour and greater than the losses when where battery and DG is integrated because EV acts as load.

(2) Topology 2. In scenario 2, the losses for each hour for each case is shown in Table 7 and the losses are high in 19th hour of the day in absence of DGs due to the presence of maximum amount of load which is 98.4633 kW for that particular hour. The loss in the presence of DGs is 59.387 kW for the 19th hour, reducing the loss by 39.68% by supplying energy to the demand. In the case 3, the loss in the presence of battery and DGs, for 19th hour is 54.042 kW, the loss is decreased by 46.13% where battery is in charging position because of this condition the losses are decreased due to load is low at that particular hour. In the next case, then only EVs are integrated in the system, the loss for 19th hour is

TABLE 6: Power loss (in kW) 33 bus system scenario 1.

Time (hours)	Topology 1					Topology 2				
	Case 1	Case 2	Case 3	Case 4	Case 5	Case 1	Case 2	Case 3	Case 4	Case 5
1	161.57	90.07	93.84	161.57	75.07	78.77	47.50	61.84	78.77	49.47
2	162.58	90.63	94.42	162.58	76.01	79.26	47.80	61.84	79.26	49.78
3	163.59	91.20	95.01	163.59	76.96	79.75	48.10	61.84	79.75	50.09
4	165.21	92.10	95.95	165.21	78.48	80.54	48.57	61.84	80.54	50.59
5	167.63	93.45	97.35	167.63	80.80	81.72	49.29	61.84	81.72	51.33
6	183.79	102.46	77.40	183.83	77.42	89.60	54.04	54.59	89.63	49.69
7	191.87	106.96	81.47	192.10	81.59	93.54	56.41	54.36	93.69	51.72
8	195.91	109.21	84.26	196.33	84.49	95.50	57.60	54.13	95.79	52.65
9	201.97	112.59	88.74	202.70	89.15	98.46	59.38	53.99	98.96	54.25
10	197.93	110.34	88.66	198.35	88.90	96.49	58.19	54.05	96.78	53.12
11	201.97	112.59	92.94	201.15	92.47	98.46	59.38	54.33	97.91	54.04
12	195.91	109.21	92.02	194.91	91.45	95.50	57.60	54.66	94.84	52.66
13	191.87	106.96	91.53	190.89	91.20	93.54	56.41	54.96	93.16	52.01
14	181.77	101.33	105.57	183.72	106.91	88.61	53.44	61.84	89.96	56.59
15	182.78	101.89	87.33	181.53	86.61	89.10	53.74	55.00	88.28	49.33
16	183.79	102.46	88.09	183.57	87.96	89.60	54.04	55.07	89.45	50.03
17	187.83	104.71	90.91	187.61	90.77	91.57	55.22	55.29	91.42	51.34
18	181.77	101.33	105.57	183.58	106.81	88.61	53.44	61.84	89.86	56.52
19	189.85	105.83	93.11	191.01	93.88	92.55	55.82	55.62	93.34	52.76
20	195.91	109.21	98.44	196.91	99.07	95.50	57.60	56.29	96.19	55.02
21	201.97	112.59	105.25	203.00	105.91	98.46	59.38	57.46	99.16	57.90
22	187.83	104.71	99.00	188.05	99.15	91.57	55.22	57.85	91.72	53.90
23	181.77	101.33	105.57	181.99	105.71	88.61	53.44	61.84	88.76	55.75
24	189.85	105.83	110.26	190.26	110.53	92.55	55.82	61.84	92.83	58.32

TABLE 7: Power loss (in kW) 33 bus system scenario 2.

Time (hours)	Topology 1					Topology 2				
	Case 1	Case 2	Case 3	Case 4	Case 5	Case 1	Case 2	Case 3	Case 4	Case 5
1	79.03	44.05	45.90	79.03	45.90	38.52	23.23	61.84	38.52	24.20
2	52.68	29.37	30.60	52.68	30.60	25.68	15.49	61.84	25.68	16.13
3	43.90	24.47	25.50	43.90	25.50	21.40	12.91	61.84	21.40	13.44
4	35.12	19.58	20.40	35.12	20.40	17.12	10.32	61.84	17.12	10.75
5	35.12	19.58	20.40	35.12	20.40	17.12	10.32	61.84	17.12	10.75
6	35.12	19.58	20.40	35.13	20.40	17.12	10.32	61.84	17.12	10.75
7	43.90	24.47	25.50	43.95	25.53	21.40	12.91	61.84	21.44	13.46
8	61.46	34.26	35.70	61.60	35.78	29.96	18.07	61.84	30.05	18.88
9	70.25	39.16	40.80	70.50	40.97	34.24	20.65	61.84	34.42	21.62
10	87.81	48.95	51.00	88.00	51.12	42.81	25.82	61.84	42.93	26.97
11	105.37	58.74	61.20	105.37	60.91	51.37	30.98	61.84	51.08	32.07
12	119.42	66.57	69.36	118.81	68.95	58.22	35.11	61.84	57.81	36.30
13	131.72	73.43	76.50	131.33	76.24	64.21	38.73	61.84	63.95	40.16
14	149.28	83.22	86.70	150.88	87.80	72.77	43.89	61.84	73.88	46.47
15	166.84	93.01	96.90	165.70	96.14	81.33	49.05	61.84	80.58	50.59
16	175.62	97.90	102.00	175.41	101.86	85.62	51.64	61.84	85.48	53.68
17	184.40	102.80	77.69	184.19	77.58	89.90	54.22	54.58	89.75	49.76
18	194.94	108.67	83.04	196.88	84.10	95.03	57.32	54.29	96.37	53.08
19	201.97	112.59	87.73	203.20	88.42	98.46	59.38	54.04	99.30	54.47
20	187.92	104.76	82.17	188.88	82.70	91.61	55.25	54.00	92.26	50.59
21	175.62	97.90	153.44	176.52	154.18	85.62	51.64	89.19	86.23	78.09
22	149.28	83.22	141.15	149.46	141.30	72.77	43.89	96.53	72.89	71.45
23	131.72	73.43	76.50	131.87	76.60	64.21	38.73	61.84	64.32	40.40
24	105.37	58.74	61.20	105.60	61.35	51.37	30.98	61.84	51.52	32.37

99.3068 kW. The loss is increased by 0.85% for the 19th hour as EV acts as load for the system. In the case 5, the losses are reduced to 54.4758 kW for 19th hour. The loss is reduced by 44.67% for 19th hour which is lesser than the losses when only DG is integrated because as discussed earlier, the battery acts as energy source and greater than the losses when battery and DG is integrated since EV acts as load.

3.2. 69 Bus System.

The power losses for 24 hours are computed for the two different loading scenarios and two different topologies on the IEEE 69 Bus system. The results are shown in Tables 8 and 9.

3.2.1. Scenario 1

(1) Topology 1. In scenario 1, the losses for each hour for each case is shown in Table 8. The losses are high in 9th, 11th, and 21st hours of the day in absence of DGs due to the presence of maximum amount of load which is 229.2533 kW for each hour, respectively. The loss in the presence of DGs is 115.4602 kW for the 9th hour, 11th hour, and 21st hour. Thereby reducing the losses by 49.63% since DG supplies the demand. In the case 3, the losses for 9th hour is 94.1565 kW, for 11th hour is 99.0057 kW and for 21st hour, the loss is 111.6846 kW, and the losses are decreased by 58.92%, 56.81%, and 51.28%, respectively. Battery is in discharging position because of this condition the losses are decreased. In the next case, only EVs are integrated in the system, the loss for 9th hour is 238.0188 kW, for the 11th hour is 220.4388 kW, and for 21st hour is 241.8434 kW. The loss is increased by 3.82% for the 9th hour as EV acts as load for the system, has decreased 3.84% for the 11th hour as EV acts as source here so the loss is decreased and has increased for 21st hour by 5.49% due to EV acts as load for the system. In the case 5, when all three EVs, batteries and DGs are integrated to the system, the losses are reduced to 99.0258 kW, 94.4265 kW, and 119.6756 kW for 9th, 11th, and 21st hour. The losses are reduced by 56.80% for 9th hour, 58.81% for 11th hour, and 47.79% for 21st hour which is lesser than the losses when only DG is integrated because either EV or battery or both acts as energy source(s).

(2) Topology 2. In scenario 1, the losses for each hour for each case are shown in Table 8. The losses are high in 9th, 11th, and 21st hours of the day in absence of DGs due to the presence of maximum amount of load which is 44.3165 kW for each hour, respectively. The loss in the presence of DGs is 27.8136 kW for the 9th hour, 11th hour, and 21st hour. Thereby reducing the losses by 39.49%. In the case 3, the losses for 9th hour is 23.0009 kW, for 11th hour is 23.7792 kW, and for 21st hour is 26.191 kW. The losses are decreased by 48.09%, 46.34%, 40.90% respectively where battery is in charging position in 21st hour because of this condition the

losses are decreased and the battery is in idle position for the 9th and 11th hour. In the case 4, the loss for 9th hour is 47.71 kW, for the 11th hour is 41.4444 kW, and for the 21st hour is 49.393 kW. The loss is increased by 7.65% for the 9th hour as EV acts as load for the system and has decreased 6.48%, for the 11th hour as EV acts as source here so the loss is decreased and has increased for 21st hour by 11.45% due to EV acts as load for the system. In the subsequent case when all three EVs, batteries and DGs are integrated to the system, the losses are reduced to 25.6346 kW, 21.9699 kW, and 30.1646 kW for 9th, 11th, and 21st hour, respectively. The losses are reduced by 42.15% for 9th hour, 50.42% for 11th hour, and 31.93% for 21st hour which are lesser than the losses when only DG is integrated because in 9th hour both EV and battery is discharging, in 11th hour, battery alone is discharging and EV acts as load but effect of EV for this hour is low, and in 21st hour, both acts as energy source.

3.2.2. Scenario 2

(1) Topology 1. In scenario 2, the losses for each hour for each case are shown in Table 9. The losses are high in 19th hour of the day in absence of DGs, due to the presence of maximum amount of load which is 229.2533 kW for that particular hour. The loss in the presence of DGs is 112.4602 kW for the 19th hour. Thereby reducing the loss by 49.63% since DG is fulfilling the demand. In the case 3, the loss for 19th hour is 92.9072 kW, the loss is decreased by 59.47% where battery is in discharging position. In the next case, the loss for 19th hour is 244.4956 kW. The loss is increased by 6.64% for the 19th hour as EV acts as load for the system. In the case 5, the losses are reduced to 101.524 kW for 19th hour, the loss is reduced by 55.71% for 19th hour which is lesser than the losses when only DG is integrated because battery is discharging and greater than the losses when battery and DG is integrated since EV acts as load.

(2) Topology 2.. In scenario 2, the losses for each hour for each case is shown in Table 9 and the losses are high in 19th hour of the day in absence of DGs due to the presence of maximum amount of load which is 44.3165 kW for that particular hour. The loss in the presence of DGs is 27.8136 kW for the 19th hour. Thereby reducing the loss by 37.23% since the DG is fulfilling the demand. In the next case, the loss in the presence of battery and DGs, for 19th hour is 22.8223 kW, the loss is decreased by 48.50% where battery is in discharging position. In the case 4, the loss for 19th hour is 50.6078 kW. The loss is increased by 14.19% for the 19th hour as EV acts as load for the system. In the subsequent case, the losses are reduced to 27.7808 kW for 19th hour. The loss is reduced by 37.31% for 19th hour which is lesser than the losses when only DG is integrated since DG alone cannot fulfill the required demand and greater than the losses when battery and DG are integrated because EV and battery, both acts as energy source.

TABLE 8: Power loss (in kW) 69 bus system scenario 1.

Time (hours)	Topology 1					Topology 2				
	Case 1	Case 2	Case 3	Case 4	Case 5	Case 1	Case 2	Case 3	Case 4	Case 5
1	183.40	92.36	98.45	183.40	98.45	35.45	22.25	28.60	35.45	22.88
2	184.54	92.94	99.07	184.54	99.07	35.67	22.38	28.60	35.67	23.02
3	185.69	93.52	99.690	185.69	99.69	35.89	22.52	28.60	35.89	23.16
4	187.52	94.44	100.67	187.52	100.67	36.25	22.75	28.60	36.25	23.39
5	190.28	95.83	102.15	190.28	102.15	36.78	23.08	28.60	36.78	23.73
6	208.62	105.06	81.24	209.12	81.49	40.32	25.31	22.38	40.42	20.49
7	217.79	109.68	85.77	220.44	87.14	42.10	26.42	22.48	43.00	22.09
8	222.37	111.99	89.04	227.34	91.69	42.98	26.97	22.67	44.80	23.40
9	229.25	115.46	94.15	238.01	99.02	44.31	27.81	23.00	47.71	25.63
10	224.66	113.15	94.29	229.68	97.07	43.43	27.25	23.31	45.26	24.27
11	229.25	115.46	99.00	220.43	94.42	44.31	27.81	23.77	41.44	21.96
12	222.37	111.99	98.07	211.86	92.60	42.98	26.97	24.14	39.72	21.42
13	217.79	109.68	97.54	211.66	94.19	42.10	26.42	24.44	39.99	21.85
14	206.32	103.91	110.76	231.71	128.39	39.88	25.03	28.60	51.30	35.02
15	207.47	104.49	93.07	194.62	86.49	40.10	25.17	24.46	36.46	20.07
16	208.62	105.06	93.87	206.18	92.51	40.32	25.31	24.52	39.39	21.71
17	213.20	107.37	96.83	210.72	95.45	41.21	25.86	24.70	40.26	22.36
18	206.32	103.91	110.76	229.66	109.23	39.88	25.03	28.60	50.24	34.12
19	215.49	108.53	99.16	229.82	114.71	41.65	26.14	24.96	47.57	28.12
20	222.37	111.99	104.71	234.58	113.99	42.98	26.97	25.44	47.91	28.53
21	229.25	115.46	111.68	241.84	119.67	44.31	27.81	26.19	49.39	30.16
22	213.20	107.37	104.95	215.80	106.61	41.21	25.86	26.43	42.10	25.29
23	206.32	103.91	110.76	208.84	112.40	39.88	25.03	28.60	40.74	26.42
24	215.49	108.53	115.69	220.31	118.84	41.65	26.14	28.60	43.42	28.25

TABLE 9: Power loss (in kW) 69 bus system scenario 2.

Time (hours)	Topology 1					Topology 2				
	Case 1	Case 2	Case 3	Case 4	Case 5	Case 1	Case 2	Case 3	Case 4	Case 5
1	89.70	45.18	48.15	89.70	48.15	17.34	10.88	28.60	17.34	11.19
2	59.80	30.12	32.10	59.80	32.10	11.56	7.25	28.60	11.56	7.46
3	49.83	25.10	26.75	49.83	26.75	9.63	6.04	28.60	9.63	6.21
4	39.87	20.08	21.40	39.87	21.40	7.70	4.83	28.60	7.70	4.97
5	39.87	20.08	21.40	39.87	21.40	7.70	4.83	28.60	7.70	4.97
6	39.87	20.08	21.40	39.96	21.46	7.70	4.83	28.60	7.72	4.99
7	49.83	25.10	26.75	50.44	27.15	9.63	6.04	28.60	9.84	6.38
8	69.77	35.14	37.45	71.33	38.47	13.48	8.46	28.60	14.05	9.14
9	79.74	40.16	42.80	82.78	44.82	15.41	9.67	28.60	16.59	10.86
10	99.67	50.20	53.51	101.90	54.96	19.26	12.09	28.60	20.08	13.06
11	119.61	60.24	64.21	115.01	61.38	23.12	14.51	28.60	21.62	13.97
12	135.55	68.27	72.77	129.14	68.87	26.20	16.44	28.60	24.21	15.69
13	149.51	75.30	80.26	145.30	77.64	28.90	18.13	28.60	27.45	17.72
14	169.44	85.34	90.96	190.29	105.44	32.75	20.55	28.60	42.13	28.76
15	189.38	95.38	101.67	177.65	94.70	36.60	22.97	28.60	33.28	21.74
16	199.35	100.40	107.02	197.02	105.54	38.53	24.18	28.60	37.64	24.30
17	209.31	105.42	81.57	206.87	80.37	40.46	25.39	22.38	39.52	19.84
18	221.27	111.44	87.51	246.30	101.93	42.77	26.84	22.53	53.89	30.73
19	229.25	115.46	92.90	244.49	101.52	44.31	27.81	22.82	50.60	27.78
20	213.30	107.42	87.12	225.01	93.71	41.23	25.87	22.92	45.95	25.02
21	199.35	100.40	151.19	210.29	159.86	38.53	24.18	40.37	42.95	38.56
22	169.44	85.34	137.21	171.51	138.87	32.75	20.55	43.19	33.46	32.49
23	149.51	75.30	80.26	151.33	81.45	28.90	18.13	28.60	29.52	19.15
24	119.61	60.24	64.21	122.28	65.96	23.12	14.51	28.60	24.10	15.68

4. Conclusion

In this work, GA was implemented to install DGs at optimal location with optimal capacity by fixing penetration level (PL) on standard IEEE 33 and 69 bus systems. The main process of GA includes selection, reproduction, crossover, and mutation. The effect of DGs in loss reduction for various topologies and load profiles were computed. The SoC value for each hour before placing the battery based on the demand was estimated, then battery was placed in the optimal location of the fixed capacity. The battery operation for each hour based on estimated SoC for various conditions were also obtained and the effect of battery operation along with DGs in reducing power losses for various conditions were also computed. Electric vehicle (EV) of fixed size in both the test systems were incorporated and also estimated the losses for various conditions. Eventually, the effect of coordinated operation of EVs along with DGs and battery for loss reduction are understood. The above-given processes were carried out for 2 topologies for different scenarios mentioned in problem formulation and estimated the corresponding losses. The future scope of this work would be estimating the losses when PV and wind turbines are installed separately for both the topologies and for different scenarios.

Abbreviation

DG: Distributed generator
GA: Genetic algorithm
PL: Penetration level
SoC: State of charge
EV: Electric vehicle
BESS: Battery energy storage system
LR: Loss reduction
DoD: Depth of discharge
LFA: Load flow analysis

Symbols

PL: Penetration level
P_{DG}: Real power generated by DGs
P_{grid}: The real power supplied by the grid to the loads in the network
LR: Loss reduction
V_t: Bus voltage measured in p.u.
V_{low}: Minimum voltage at the bus (0.95 p.u.)
V_{high}: Maximum voltage at the bus (1.05 p.u.)
S_{line}: Power flow in the line
S_{high}: Maximum allowable power flow in the line
x_1: PL
x_2: Location index
x_3: Type of DG
X: Population matrix
P: Total population
p_i: Parent i
p_j: Parent j
o_i: Child i
o_j: Child j
k: Selected crossover point

m: Mutant child
E: Energy of the battery
∂_y: Time interval
η_d: Discharging efficiency
η_c: Charging efficiency
$SoC(y)$: State of charge in present hour
$SoC(y-1)$: State of charge in previous hour
P_{batt}: Output power of e battery
SoC_{min}: Minimum SoC
SoC_{max}: Maximum SoC.

Data Availability

Previously reported data were used to support this study and are cited at relevant places within the text as references [8, 15, 16, 19, 20].

Disclosure

This paper is an extended version of our published paper: Iyer, Kartik, J. Mounikaa, Misha Jha, K. Narayanan, Gulshan Sharma, Anurag Sharma, and Tomonobu Senjyu, "Power loss reduction in distribution systems in the presence of DGs and EVs." IEEE PES Innovative Smart Grid Technologies-Asia (ISGT Asia), (2022). pp. 680–684, doi: 10.1109/ISGTAsia54193.2022.10003589.

Conflicts of Interest

The authors declare that they have no conflicts of interest regarding the publication of this paper.

References

[1] M. Khosravi, S. Afsharnia, and S. Farhangi, "Optimal sizing and technology selection of hybrid energy storage system with novel dispatching power for wind power integration," *International Journal of Electrical Power & Energy Systems*, vol. 127, Article ID 106660, 2021.

[2] M. H. Moradi and M. Abedini, "A combination of genetic algorithm and particle swarm optimization for optimal DG location and sizing in distribution systems," *International Journal of Electrical Power & Energy Systems*, vol. 34, no. 1, pp. 66–74, 2012.

[3] S. Solat, F. Aminifar, and H. Shayanfar, "Distributed generation hosting capacity in electric distribution network in the presence of correlated uncertainties," *IET Generation, Transmission & Distribution*, vol. 15, no. 5, pp. 836–848, 2020.

[4] A. Uniyal and S. Sarangi, "Optimal network reconfiguration and DG allocation using adaptive modified whale optimization algorithm considering probabilistic load flow," *Electric Power Systems Research*, vol. 192, Article ID 106909, 2021.

[5] P. Priyanka, "Comprehensive analysis of distributed energy resource penetration and placement using probabilistic framework," *IET Renewable Power Generation*, vol. 15, no. 4, 2020.

[6] A. Ali, M. U Keerio, and J. A Laghari, "Optimal site and size of distributed generation allocation in radial distribution network using multi-objective optimization," *Journal of modern Power Systems and Clean Energy*, vol. 9, no. 2, pp. 404–415, March 2021.

[7] M. Khasanov, S. Kamel, H. M. Hasanien, and A. Al-Durra, "Rider optimization algorithm for optimal DG allocation in radial distribution network," in *Proceedings of the 2nd International Conference on Smart Power & Internet Energy Systems (SPIES)*, Bangkok, Thailand, September, 2020.

[8] T. Rawat, K. R. Niazi, N. Gupta, and S. Sharma, "Impact analysis of demand response on optimal allocation of wind and solar based distributed generations in distribution system," *Energy Sources, Part B: Economics, Planning and Policy*, vol. 16, no. 1, pp. 75–90, 2021.

[9] D. Kumar, S. R. Samantaray, I. Kamwa, and N. C. Sahoo, "Reliability-constrained based optimal placement and sizing of multiple distributed generators in power distribution network using Cat swarm optimization," *Electric Power Components and Systems*, vol. 42, no. 2, pp. 149–164, 2014.

[10] A. Rezaee Jordehi, M. S. Javadi, and J. P S Catalão, "Optimal placement of battery swap stations in microgrids with micro pumped hydro storage systems, photovoltaic, wind and geothermal distributed generators," *International Journal of Electrical Power & Energy Systems*, vol. 125, Article ID 106483, 2021.

[11] M. Amini, A. Khorsandi, B. Vahidi, S. H. Hosseinian, and A. Malakmahmoudi, "Optimal sizing of battery energy storage in a microgrid considering capacity degradation and replacement year," *Electric Power Systems Research*, vol. 195, Article ID 107170, 2021.

[12] G. K. Zaher, M. F. Shaaban, M. Mokhtar, and H. H. Zeineldin, "Optimal operation of battery exchange stations for electric vehicles," *Electric Power Systems Research*, vol. 192, Article ID 106935, 2021.

[13] P. Rajesh and F. H. Shajin, "Optimal allocation of EV charging spots and capacitors in distribution network improving voltage and power loss by Quantum-Behaved and Gaussian Mutational Dragonfly Algorithm (QGDA)," *Electric Power Systems Research*, vol. 194, Article ID 107049, 2021.

[14] S. K. R. Moupuri and K. Selvajyothi, "Optimal planning and utilisation of existing infrastructure with electric vehicle charging stations," *IET Generation, Transmission & Distribution*, vol. 15, no. 22, p. 1510, 2020.

[15] K. Iyer, J. Mounikaa, M. Jha et al., "Power loss reduction in distribution systems in the presence of DGs and EVs," in *Proceedings of the IEEE PES Innovative Smart Grid Technologies-Asia (ISGT Asia)*, pp. 680–684, Singapore, November, 2022.

[16] K. Chellappan, V. S. S. C. S. Murty, N. Krishnan, G. Sharma, and T. Senjyu, "Real power loss minimization considering multiple DGs and battery in distribution system," *Electric Power Components and Systems*, vol. 49, no. 6-7, pp. 563–572, 2021.

[17] M. Mahoor, Z. S. Hosseini, and A. Khodaei, "Least-cost operation of a battery swapping station with random customer requests," *Energy*, vol. 172, pp. 913–921, 2019.

[18] S. Singh, P. Chauhan, and N. Jap Singh, "Feasibility of grid-connected solar-wind hybrid system with electric vehicle charging station," *Journal of modern Power Systems and Clean Energy*, vol. 9, no. 2, pp. 295–306, March 2021.

[19] K. S. P. V. S. Nihith, V. Shivkumar, N. Krishnan, G. Sharma, and T. Senjyu, "Voltage stability analysis of distribution systems in presence of electric vehicle charging stations with coordinated charging scheme," *International Transactions on Electrical Energy Systems*, vol. 31, Article ID 13248, 2021.

[20] R. S. Rao, K. Ravindra, K. Satish, and S. V. L. Narasimham, "Power loss minimization in distribution system using network reconfiguration in the presence of distributed generation," *IEEE Transactions on Power Systems*, vol. 28, no. 1, pp. 317–325, 2013.

[21] S. Ghore, P. Das, and M. Biswal, "Uninterrupted power supply to BESS based microgrid system using adaptive reclosing approach," *IET Generation, Transmission & Distribution*, vol. 15, no. 7, pp. 1203–1213, 2020.

[22] M. Mohseni, M. Joorabian, and A. Lashkar Ara, "Distribution system reconfiguration in presence of Internet of things," *IET Generation, Transmission & Distribution*, vol. 15, no. 8, pp. 1290–1303, 2020.